

Structure of liquid water under high pressure up to 17 GPa

Yoshinori Katayama, Takanori Hattori, Hiroyuki Saitoh, Takashi Ikeda, and Katsutoshi Aoki
 Synchrotron Radiation Research Center, Japan Atomic Energy Agency, Kouto 1-1-1, Sayo, Hyogo 679-5148, Japan

Hiroshi Fukui*

Institute for Study of the Earth's Interior, Okayama University, Misasa, Tottori 682-0193, Japan

Kenichi Funakoshi

Japan Synchrotron Radiation Research Institute, Kouto 1-1-1, Sayo, Hyogo 679-5198, Japan

(Received 3 November 2009; revised manuscript received 14 December 2009; published 20 January 2010)

The structure of liquid water was studied along the melting curve up to 17.1 GPa and 850 K by *in situ* x-ray diffraction. Because an oxygen atom has a much larger x-ray scattering power than that of a hydrogen atom, pressure dependence of local molecular arrangements was revealed straightforwardly. At low pressures, the local structure changed toward a simple liquidlike structure through an increase in the coordination number of water molecules. Once densely packed structure was achieved around 4 GPa, the volume was reduced through the decrease in the intermolecular distance on further compression. Classical molecular-dynamics simulations well reproduced the experimental results although the degree of agreement depended on pressure. Limitations of the pair-potential model were discussed.

DOI: [10.1103/PhysRevB.81.014109](https://doi.org/10.1103/PhysRevB.81.014109)

PACS number(s): 64.70.Ja, 61.25.Em, 62.50.-p

I. INTRODUCTION

The structure of water and its pressure variations have been widely studied because they are crucial for understanding the unusual properties of water.¹⁻¹⁷ In ordinary ice (ice Ih), each water molecule forms hydrogen bonds with four nearest-neighbor molecules in the tetrahedral position. This relatively open network structure shows a remarkably rich response to pressure and temperature: there are at least 13 crystalline phases and three distinct amorphous forms. Figure 1 shows the phase diagram of water.^{1,18} At low pressures, below 0.6 GPa, a denser packing of water molecules in high-pressure crystalline phases has been realized through the distortion of the tetrahedral local structure and the closer approach of non-nearest neighbors.¹ The main difference among low-density (LDA), high-density (HDA), and very high-density amorphous (VHDA) ices also appears in the number of nonbonding molecules that move close to the first shell.²⁻⁵ In liquid water at ambient conditions, the tetrahedral local structure is essentially preserved, although distorted.⁶⁻⁹ Structural studies on liquid water at moderate pressures have revealed that a closer approach of nonbonding molecules is again significant.¹⁰⁻¹⁶

A different mechanism for densification dominates at higher pressures. In ice VII, which is stable above 2.1 GPa, the oxygen atoms form a body-center cubic (bcc) sublattice. This densely packed structure consists of two interpenetrating diamondlike hydrogen-bonded lattices. In this phase, volume reduction under compression is achieved by a decrease in the intermolecular distance. A first-principles molecular-dynamics (FPMD) simulation study has shown that liquid water at 10 GPa also exhibits a large coordination of oxygen atoms.¹⁹ A recent neutron-scattering study on heavy water has supported this prediction.²⁰ The reported oxygen-oxygen (O-O) pair-correlation function at 6.5 GPa and 670 K, the highest pressure in the study, is strikingly similar to that of liquid Ar, which can be described by random packed spheres.

It is not, however, trivial to obtain an O-O partial structure from neutron scattering because the contribution of O-O pairs to the total scattering is less than 9%. The O-O partial structure reported in the aforementioned study²⁰ was obtained with a help of a Monte Carlo simulation based on a classical water model (empirical potential structural refinement method) (Refs. 9-11): an initial structural model was constructed by a simulation using the extended simple point charge model (SPC/E) reference potential and the model was refined by perturbing the potential so as to reproduce the experimental data. In contrast to the neutron case, determination of O-O partial structure is straightforward in the x-ray case because an oxygen atom has a much larger x-ray scattering power than that of a hydrogen atom. In fact, recent x-ray diffraction measurements up to 57 GPa using a laser-heated diamond-anvil cell have confirmed a simple liquidlike structure at high pressures.^{21,22} But agreement between the experimental and theoretical structure factors is only qualitative partly due to a large uncertainty in temperature.^{21,22} To

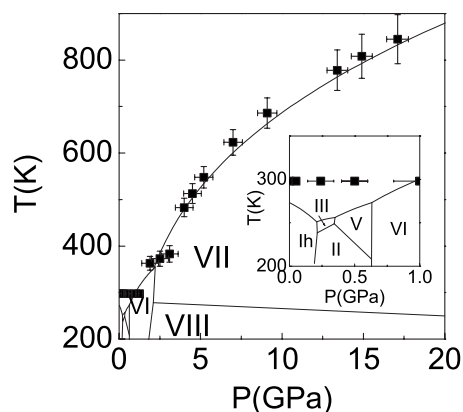


FIG. 1. Phase diagram of water with points where measurements were conducted. Inset shows the low-pressure region.

investigate the packing of water molecules under compression in detail, we have carried out *in situ* x-ray diffraction experiments on liquid water under high pressure up to 17.1 GPa using large volume presses. MD simulations on a classical SPC/E model have also been performed for comparison.

II. EXPERIMENTAL AND COMPUTATIONAL DETAILS

X-ray diffraction experiments up to 9.1 GPa were carried out using a single-stage cubic-type multianvil press installed on BL14B1 while those above 9.1 GPa were carried out using a Kawai-type double-stage press installed on BL04B1 at the SPring-8 synchrotron radiation facility.²³ The sample was deionized water. A single-crystal diamond cup was used as the sample container because diamond is liquid tight, x-ray transparent, and chemically stable. Pressure was transmitted through a cap made of gold (up to 9.1 GPa) or platinum (above 9.1 GPa). The sample container was inserted into a graphite tube heater, which was placed in a pressure-transmitting medium made of a mixture of boron and epoxy resin. The pressure was determined by a NaCl pressure marker (up to 9.1 GPa) (Ref. 24) or Pt (above 9.1 GPa).²⁵ The temperature was estimated from the power applied to the heater, where the power-temperature relation was calibrated by the melting curve of water reported in the literature.¹⁸ Diffraction data were collected by an energy-dispersive method. X-ray scattering from the empty cell was measured beforehand and subtracted from the data. The incoherent scattering was subtracted based on results of a theoretical calculation.²⁶ Structure factor, $S(Q)$, was determined from a set of diffraction patterns measured at different diffraction angles using an empirical method.^{27,28} To obtain O-O correlation, a molecular form factor²⁶ was used according to the previous studies.⁶⁻⁸ The structure factor was corrected by subtracting the inverse Fourier transform of the unphysical oscillations in low- r region of the pair-correlation function, $g(r)$.²⁹ The density, ρ , at each P - T point was calculated using IAPWS-95 formulation.³⁰

Classical MD simulations were performed on a sample of 4096 water molecules using a code MDYNAMIX.³¹ The SPC/E model³² was employed because it was simple and popular and because it was used as an intermolecular reference potential to obtain structural data in the previous neutron-scattering study.²⁰ Flexibility of the molecules was introduced using a method in Ref. 33. Because it is not certain if the model reproduces the equation of state of water, the simulations were performed under constant volume and constant temperature conditions using calculated ρ at each P - T point.

III. RESULTS

The measurements were conducted just above the melting temperature at each pressure as shown in Fig. 1. Figure 2 shows $S(Q)$ of water at selected pressures up to 17.1 GPa [thick solid (black) line]. The structure factor under ambient conditions agrees well with the previously reported one, which is indicated by a dashed line.⁸ The structure factor has

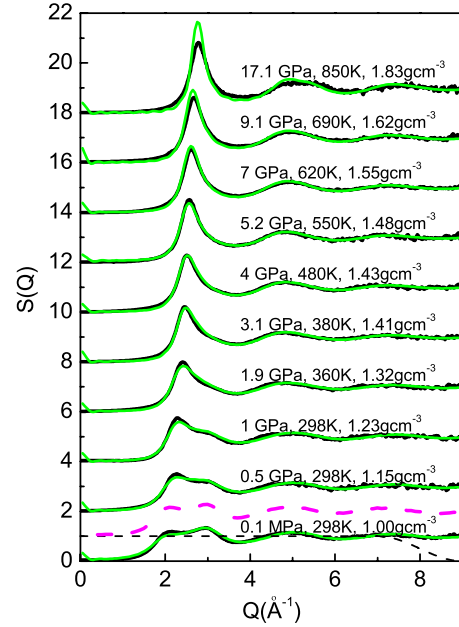


FIG. 2. (Color online) Molecular structure factor, $S(Q)$, at various pressures and temperatures. Thick solid lines (black) indicate $S(Q)$ obtained by the present x-ray diffraction experiments. Dashed (violet) line indicates $S(Q)$ at ambient conditions reported in the literature (Ref. 8). Solid gray (green) lines indicate results of classical MD simulations, obtained by Fourier transformation of the simulated O-O pair-correlation function. Dotted (black) line indicates window function used for the Fourier transformation of $S(Q)$ to obtain pair-correlation function.

a characteristic double peak structure ($1.5 < Q < 3.5 \text{ \AA}^{-1}$) in the vicinity of the principal peak of simple liquids. This doublet structure is a signature of the open network structure: similar doublet structure is observed in other materials that have open-packed structure such as amorphous and liquid Si.³⁴⁻³⁶ It is possibly related to separation of interstitial voids.^{34,35} As the pressure increases, the intensity of the first peak increases and its position shifts to a higher Q , but the second peak becomes less prominent. The second peak becomes a shoulder of a first peak around 3.1 GPa ($\rho = 1.41 \text{ g cm}^{-3}$) and vanishes near 5.2 GPa ($\rho = 1.48 \text{ g cm}^{-3}$). In the same pressure range, the intensity of the oscillations in the high Q region above 4 \AA^{-1} gradually increase. Structure factor becomes similar to that of a simple liquid. Upon further compression, all peaks shift to higher Q 's.

Figure 3 shows the corresponding $g(r)$ that was obtained by a Fourier transformation [thick solid (black) line]. Because scatter of $S(Q)$ in the high- Q region ($Q > 8 \text{ \AA}^{-1}$) is large, $S(Q)$ up to 9 \AA^{-1} was transformed using an extended cosine-bell window function, which is shown by the thin dotted (black) line in Fig. 2. The first peak at 2.85 \AA corresponds to the O-O nearest-neighbor correlation. Due to the limited Q range of $S(Q)$, termination ripples appear in both sides of the first peak. The position of the second peak is about 4.5 \AA , and the ratio of the position of the second peak to that of the first peak is about 1.6, which is close to the value for the tetrahedral arrangement, 1.63. At 0.5 GPa ($\rho = 1.15 \text{ g cm}^{-3}$), the second peak and the dip between the first

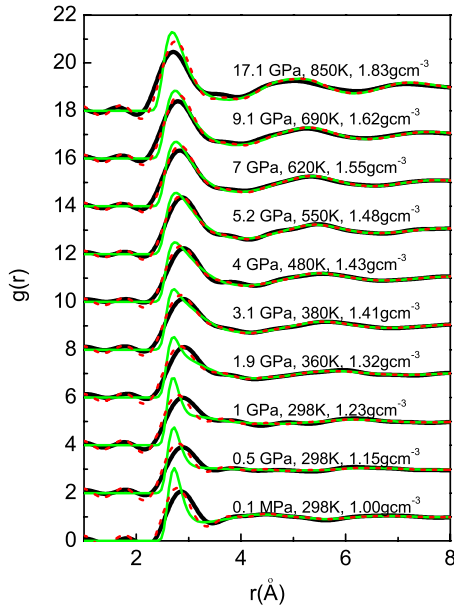


FIG. 3. (Color online) Pair-correlation function, $g(r)$, at various pressures and temperatures. Thick solid lines (black) indicate experimental results. Solid gray (green) lines indicate O-O pair-correlation functions obtained by classical MD simulations. Dotted (red) lines indicate theoretical O-O pair-correlation functions after broadening by the experimental resolution function. See text for details.

and the second peaks nearly vanished. At 1 GPa, the intensity at the large- r side of the first peak increases and the first peak becomes asymmetric. Above 1.9 GPa ($\rho = 1.32 \text{ g cm}^{-3}$), the first peak becomes symmetric again as the intensity at the large- r side of the first peak begins to decrease, while a new second peak simultaneously develops between 4 and 7 Å. The position of the second peak is about 5.5 Å at 5.2 GPa, and the ratio of the position of the second peak to that of first peak is 1.9. The value is much larger than that at ambient pressure but is typical for a simple liquid.³⁶ Above 5.2 GPa, all peaks gradually shift to smaller r 's keeping their overall shape.

IV. DISCUSSION

The observed features in the pressure dependence of $S(Q)$ and $g(r)$ reveal that the volume reduction in a low-pressure range below 4 GPa is accompanied by a drastic change in local molecular arrangement. At ambient conditions, tetrahedral local structure due to hydrogen bonding is essentially preserved in the liquid state. Hence water has relatively open structure with interstitial empty spaces. The disappearance of the second peak and the dip between the first and the second peaks in $g(r)$ at 0.5 GPa indicate that part of the molecules in the second shell move toward the first shell and fill the empty spaces. Subsequent compression increases the intensity at the large- r side of the first peak: the inward shift of the second shell continues.

To elucidate pressure dependence of the local structure, we plot the position of the first peak, r_1 , in $g(r)$ and the coordination number, N_1 , of molecules as a function of pres-

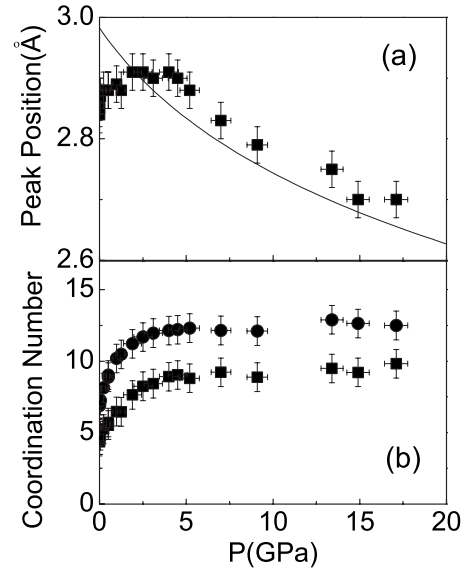


FIG. 4. (a) Pressure dependence of the position of the first peak, r_1 , in $g(r)$. Solid line indicates O-O distance in ice VII at room temperature (Ref. 33). (b) Pressure dependence of the coordination number, N_1 , of water molecules calculated by two different methods. Closed squares indicate twice the integrated value of radial distribution function, RDF, up to the maximum of the first peak in RDF. Closed circles indicate value obtained by integration of RDF up to $1.35r_1$, an estimate of the minimum position between the first and the second peaks in RDF.

sure in Figs. 4(a) and 4(b), respectively. The coordination number was calculated by two different methods. The most popular method to calculate N_1 is integration to the first minimum in $\text{RDF} = 4\pi r^2 \rho g(r)$.³⁶ In the present case, however, the minimum is not well defined due to the strong overlap of the first and second peaks as well as the termination ripple. It is especially difficult to determine the minimum position in the pressure range between 0.5 and 1.9 GPa, where the dip between the first and the second peak is shallow. To avoid the uncertainty in determining the minimum position, we used the position of the first peak to calculate N_1 . In the first method, N_1 was determined as twice the integrated value of radial distribution function (RDF) up to the maximum of the first peak in RDF (solid squares).³⁶ This method is also popular and usually gives smaller numbers compared to the integration to the first minimum in RDF. In the second method, we estimated the position of the minimum between the first and the second peak from the position of the first peak. At high pressures, the minimum roughly coincides with the distance r_1 multiplied by 1.35. Therefore we integrated RDF to $1.35r_1$ at each pressure to obtain N_1 (solid circles). This method gives reasonable estimates above ~ 4 GPa, although it overestimates the minimum position at low pressures where the minimum is closer to the first peak.

The extension of the pressure range in the present study reveals a crossoverlike behavior of two volume-reduction mechanisms. As the pressure increases, r_1 shifts slightly to larger r to about 1.9 GPa, but then remains constant up to 4 GPa. This behavior is in contrast to that observed in a simple liquid, in which the position of the first peak shifts proportionally to $(V/V_0)^{1/3}$.³⁷ In this pressure region, the volume

reduction is caused by a rapid increase in the coordination number. Above 4 GPa, the increase in the coordination number becomes saturated, and r_1 begins to shift to a smaller r . The saturated value of N_1 is ~ 9 (first method) or ~ 12 (integration to $1.35r_1$), which reaches the typical coordination number for simple liquids. For example, N_1 for noble-gas liquids is 8–9 (first method) or 10–11 (integration to the minimum) (Ref. 38) and N_1 for liquid Cu is 10.3 (first method) or 11.3 (integration to the minimum).³⁶ The shift of r_1 above 4 GPa shows that the volume is reduced through the decrease in the intermolecular distance once a densely packed structure is achieved by the closer approach of the second shell. The solid line in Fig. 4(a) indicates the pressure dependence of the O-O nearest-neighbor distance in the ice VII phase at room temperature.³⁹ In the ice VII phase, oxygen atoms form bcc sublattice and each oxygen atom has eight nearest-neighbor oxygen atoms. The peak position shifts in parallel with the O-O distance for the crystalline counterpart. This fact supports that the liquid structure contracts almost uniformly similar to a solid in this pressure range. The pressure at which crossoverlike behavior observed is higher than the transition pressure to ice VII phase in the solid state: the transformation to a dense-packed structure occurs continuously in a wide pressure range in the liquid state.

The present results agree with results of previous studies at pressures below 1 GPa that revealed that a closer approach of nonbonding molecules was significant.^{10–16} Our results also confirm a notion that the simple-liquidlike structure is realized at higher pressures proposed by previous FPMD simulation (Ref. 19) and neutron scattering (Ref. 20) studies. The FPMD simulation study at 1.57 g cm^{-3} and 600 K shows that the position of the first maximum in O-O correlation function, $g_{\text{OO}}(r)$, exhibits only a small inward shift ($\sim 0.1 \text{ \AA}$) as pressure is applied. The coordination number at 1.57 g cm^{-3} and 600 K is reported as $N_1=12.9$ when RDF is integrated to the first minimum at $r=3.94 \text{ \AA}$ and $N_1\sim 8$ when the symmetric part of the peak, i.e., up to $r=3.2 \text{ \AA}$, is integrated. These values are in excellent agreement with our results at 1.55 g cm^{-3} and 620 K, N_1 (up to 3.94 \AA) = 13.0 and N_1 (up to 3.2 \AA) = 7.9. Because $g_{\text{OO}}(r)$ reported in the neutron-scattering study is obtained with a help of a Monte Carlo simulation based on a classical water model, they are free from broadening due to the limited Q range of experimental $S(Q)$. Therefore direct comparison with our results, which are obtained by a simple Fourier transformation and thus significantly broadened, is not meaningful. Even though the reported $g_{\text{OO}}(r)$ for 6.5 GPa and 670 K, which is strikingly similar to that of liquid argon, is also very similar to the present $g(r)$ for 7 GPa and 620 K. The reported N_1 , 12 for 6.5 GPa and 670 K, which is obtained by integration up to 3.8 \AA , is also in excellent agreement with our results, N_1 (up to 3.8 \AA) = 12.0 at 7 GPa.

The slight increase in r_1 between 0.1 MPa and 2 GPa is attributed to the penetration of nonhydrogen-bonded molecules in the first shell. The elongation of the O-O nearest-neighbor distance has also been reported in the high-pressure solid phases. For example, the nearest-neighbor distance in ice VII is about 2.9 \AA at 2.5 GPa, which is much larger than that in normal ice (Ih), 2.76 \AA . Moreover a recent x-ray

study on amorphous ices has reported that the nearest-neighbor distances are 2.75 , 2.80 , and 2.83 \AA for LDA, HDA, and VHDA, respectively, at ambient pressure.⁴ To accommodate a large coordination number, expansion of the first nearest-neighbor oxygen shell is probably necessary.

The monotonous increase in N_1 with increasing pressure at low-pressure region suggests that the nonhydrogen-bonded molecules continuously penetrate into the first shell. In contrast, the nonhydrogen-bonded molecules do not penetrate into the first shell in high-pressure crystalline phases until the transition to ice VII. In ice VI, which is stable above 0.6 GPa and transforms to ice VII at 2.1 GPa, every water molecule has eight closest nonhydrogen-bonded neighbors at a distance of $\sim 3.4 \text{ \AA}$ (at 1.1 GPa and 225 K).⁴⁰ The corresponding molecules must be distributed in a wider r range in the liquid state because there is no prominent peak at $\sim 3.4 \text{ \AA}$ in $g(r)$ in this pressure range. The local structure of liquid water is much more disordered than that in the ice VI phase in which fourfold hydrogen bonding is perfectly maintained. This result is consistent with the report that the local order of supercompressed water at 1.8 GPa at room temperature is more similar to ice VII than ice VI.⁴¹ This conclusion was derived from observation of ice VII crystallized from the supercompressed water within the stability field of ice VI. The large difference in the local structure between the liquid and the stable high-pressure crystalline phases below the transition pressure to ice VII is probably related to the existence of several metastable high-pressure crystalline and glassy phases of water in this pressure range.

A contraction of the second-neighbor coordination shell with increasing pressure was also reported in a neutron-scattering study on HDA.⁵ The second peak in $g_{\text{OO}}(r)$ for HDA is centered at 3.7 \AA and this peak moves rapidly to lower r with pressure so that by 2.2 GPa it is a shoulder on the first peak at 2.8 \AA . The authors of the paper concluded that HDA had a configuration which was very like that found in ices VII and VIII. A direct comparison between the reported $g_{\text{OO}}(r)$ and our results is again difficult because the reported $g_{\text{OO}}(r)$ was obtained with a help of a Monte Carlo simulation. Even though, the similarity between the reported $g_{\text{OO}}(r)$ and our results confirm close resemblance between HDA and liquid water.⁵

Structural study of liquids under extreme conditions is still an experimental and theoretical challenge. Comparison between experimental and theoretical studies is useful to assess reliability as well as limitations of them. Thin solid gray (green) lines in Fig. 3 show O-O pair-correlation function obtained by the classical MD simulations on a sample of 4096 water molecules using the SPC/E model. They well reproduce the experimental results although there are some notable disagreements. At low pressures below 2 GPa, the first peak in theoretical $g(r)$ is much higher than the experiment. The theoretical peak is also asymmetric and shifts inward relative to the experimental peak. These differences are partly due to limited resolution of experimental $g(r)$ caused by the narrow Q range of $S(Q)$. To compare experimental and simulation results properly, we calculate $S(Q)$ of simulated water by Fourier transformation of $g(r)$. The size of the simulation box is $40 \times 40 \times 40 \text{ \AA}^3$ at the highest pressure. Therefore $g(r)$ up to 20 \AA is used for the Fourier transfor-

mation at each pressure. Because the r range of $g(r)$ in the present simulation is much larger than Q range of $S(Q)$ in the experiments ($Q < 9 \text{ \AA}^{-1}$), the resolution of calculated $S(Q)$ is better than that of experimental $g(r)$. In addition, termination ripples in calculated $S(Q)$ are negligibly small. Comparison in $S(Q)$ is thus more reliable. Thin solid gray (green) lines in Fig. 2 indicate results of the simulation. There is a small discrepancy at ambient conditions. For example, the first peak of simulated $S(Q)$ is smaller than that of experimental $S(Q)$. This discrepancy indicates that the difference between the theoretical and experimental $g(r)$ cannot be ascribed to the low resolution of the experimental $g(r)$ only. As the pressure increases, the difference becomes smaller and the agreement is excellent in the pressure range between 3 and 7 GPa. The agreement becomes worse again in the pressure range above 7 GPa. The first peak in simulated $S(Q)$ is larger than that of experimental $S(Q)$.

To include experimental resolution function in theoretical $g(r)$, the theoretical $S(Q)$ is transformed to $g(r)$ using the same window function [dotted (black) line in Fig. 3] used for the transformation of the experimental data. Dotted (red) lines in Fig. 3 indicate the broadened $g(r)$. There remain differences between experimental and theoretical $S(Q)$ after the broadening. The first peak in the broadened $g(r)$ at ambient conditions is still slightly sharper than the experimental peak and its position shifts inward relative to the experimental peak. These differences are attributable to imperfection of the simulation: the same differences between the SPC/E water and the experiment at ambient conditions have been reported in earlier studies.³² It is attributed to hardness of the repulsive term of the classical potential.^{9,32} The problem of “overstructure” is common in simulations of liquid water. The first peak in $g(r)$ of FPMD water at ambient conditions is also higher than that in experimental $g(r)$. In addition, the second peak and the dip between the first and second peak in FPMD water are more pronounced.^{42,43} It was reported that inclusion of nuclear quantum effect of hydrogen⁴² and that of empirical van der Waals corrections⁴³ in the FPMD simulations improved the agreement.

As the pressure (and also the temperature) increases, the differences become smaller and the agreement between the broadened theoretical $g(r)$ and experimental $g(r)$ is excellent in the pressure range between 3 and 7 GPa. The good agreement suggests that the local structure in this pressure range is mainly determined by the dense packing of the molecules. The hydrogen bonding, which cannot be fully represented by the simple model, is less relevant to the structure and the repulsive term plays an important role. As mentioned above, the agreement between the experimental result and FPMD simulation at 1.57 g cm^{-3} (Ref. 19) is also excellent, suggesting difficulty in describing the hydrogen bonding.

The agreement becomes worse again at high pressures at 9 GPa and above. The first peak in the theoretical $g(r)$ is significantly higher than that of experimental $g(r)$ and it shifts outward relative to the experiment. Previous studies indicated that the r^{-12} repulsive term is harder than the actual potential.^{9,34} The effect of the hard repulsive term must be more prominent in the strong compression regime. In fact, a

small reduction in the size of the diameter of the repulsive core (rough estimations: -1% at 9 GPa and -3% at 17 GPa) improves the agreement between the theory and the experiment. The other possible cause for the difference is the pressure-induced change in electronic structures. A small increase in charge transfer from hydrogen to oxygen (rough estimations: 6% at 9 GPa and 15% at 17 GPa) also improves the agreement.

The pressure dependence of O-O partial structure reported in the previous neutron-scattering study²⁰ is similar to that of SPC/E water. In the study, the partial structures were obtained with a help of a Monte Carlo simulation based on the SPC/E model: an initial structural model was constructed by a simulation using the SPC/E reference potential and the model was refined by perturbing the potential so as to reproduce the experimental data. Authors of the study indicated that the first peak in O-O partial at ambient conditions was higher than those reported previously. This disagreement suggests a possibility that O-O partial is not sufficiently refined by neutron data for heavy water only. Even though, the present results indicate that the SPC/E model is a good reference between 3 and 7 GPa as far as O-O partial structure is concerned. A joint structural refinement of x-ray and neutron data is desirable for further discussion.

V. CONCLUSION

We have measured *in situ* x-ray diffraction of liquid water up to 17.1 GPa and 850 K along the melting curve. The coordination number of molecules increases rapidly to the value for a simple liquid whereas the intermolecular nearest-neighbor distance remains almost constant below 4 GPa. However, once the densely packed structure is realized, the nearest-neighbor distance begins to decrease. The structure factors are well reproduced by a classical MD simulation although the agreement is less satisfactory in low- and high-pressure regions. The good agreement between the experiment and the theory in the middle pressure range suggests that the local structure is mainly determined by dense packing of the molecules while the disagreement in the high-pressure region is attributable to the hard repulsive term of the pair potential.

Note added in proof. An x-ray diffraction study on water up to 4.5 GPa was published recently.⁴⁴

ACKNOWLEDGMENTS

We thank A. Yoshigoe for providing the water sample, A. Nozawa for his technical support, S. Klotz and I. Goncharov for discussion. This work was supported by Grant-in-Aid for Scientific Research (C) (Grant No. 16540374) from Japan Society for the Promotion of Science, Grant-in-Aid for Scientific Research on Innovative Areas (Grant No. 20103004) from the Ministry of Education, Culture, Sports, Science and Technology of Japan, and a grant from The Mitsubishi Foundation. The experiments on BL04B1 were performed with the approval of the Japan Synchrotron Radiation Research Institute (Proposals No. 2005A0582 and No. 2005B0567).

- *Present address: School of Science, University of Hyogo, Kouto 3-2-1, Kamigori, Hyogo 678-1297, Japan.
- ¹D. Eisenberg and W. Kauzmann, *The Structure and Properties of Water* (Oxford University Press, New York, 1969).
 - ²J. L. Finney, A. Hallbrucker, I. Kohl, A. K. Soper, and D. T. Bowron, *Phys. Rev. Lett.* **88**, 225503 (2002).
 - ³J. L. Finney, D. T. Bowron, A. K. Soper, T. Loerting, E. Mayer, and A. Hallbrucker, *Phys. Rev. Lett.* **89**, 205503 (2002).
 - ⁴M. Guthrie, C. A. Tulk, C. J. Benmore, and D. D. Klug, *Chem. Phys. Lett.* **397**, 335 (2004).
 - ⁵S. Klotz, G. Hamel, J. S. Loveday, R. J. Nelmes, M. Guthrie, and A. K. Soper, *Phys. Rev. Lett.* **89**, 285502 (2002).
 - ⁶A. H. Narten and H. A. Levy, *J. Chem. Phys.* **55**, 2263 (1971).
 - ⁷F. Hajdu, S. Lengyel, and G. Pálinkás, *J. Appl. Crystallogr.* **9**, 134 (1976).
 - ⁸G. Hura, J. M. Sorenson, R. M. Glaeser, and T. Head-Gordon, *J. Chem. Phys.* **113**, 9140 (2000).
 - ⁹A. K. Soper, *J. Phys.: Condens. Matter* **19**, 335206 (2007).
 - ¹⁰A. K. Soper and M. A. Ricci, *Phys. Rev. Lett.* **84**, 2881 (2000).
 - ¹¹A. K. Soper, *Chem. Phys.* **258**, 121 (2000).
 - ¹²M. C. Bellissent-Funel and L. Bosio, *J. Chem. Phys.* **102**, 3727 (1995).
 - ¹³A. V. Okhulkov, Yu. N. Demianets, and Yu. E. Gorbaty, *J. Chem. Phys.* **100**, 1578 (1994).
 - ¹⁴J. Eggert, G. Weck, and P. Loubeyre, *J. Phys.: Condens. Matter* **14**, 11385 (2002).
 - ¹⁵J. Urquidi, S. Singh, C. H. Cho, and G. W. Robinson, *Phys. Rev. Lett.* **83**, 2348 (1999).
 - ¹⁶F. W. Starr, F. Sciortino, and H. E. Stanley, *Phys. Rev. E* **60**, 6757 (1999).
 - ¹⁷P. G. Debenedetti, *J. Phys.: Condens. Matter* **15**, R1669 (2003).
 - ¹⁸F. Datchi, P. Loubeyre, and R. LeToullec, *Phys. Rev. B* **61**, 6535 (2000).
 - ¹⁹E. Schwegler, G. Galli, and F. Gygi, *Phys. Rev. Lett.* **84**, 2429 (2000).
 - ²⁰Th. Strässle, A. M. Saitta, Y. Le Godec, G. Hamel, S. Klotz, J. S. Loveday, and R. J. Nelmes, *Phys. Rev. Lett.* **96**, 067801 (2006).
 - ²¹A. F. Goncharov, C. Sanloup, N. Goldman, J. C. Crowhurst, L. E. Fried, N. Guignot, M. Mezouar, and Y. Meng, in *Materials Research at High Pressure*, MRS Symposia Proceedings No. 987, edited by M. R. Manaa, A. F. Goncharov, R. J. Hemley, and R. Bini (Material Research Society, Warrendale, PA, 2007), p. 0987-PP04-03.
 - ²²A. Goncharov, C. Sanloup, N. Goldman, J. C. Crowhurst, S. Bastea, W. M. Howard, L. E. Fried, N. Guignot, M. Mezouar, and Y. Meng, *J. Chem. Phys.* **130**, 124514 (2009).
 - ²³N. Funamori and K. Tsuji, *Phys. Rev. B* **65**, 014105 (2001).
 - ²⁴D. L. Decker, *J. Appl. Phys.* **36**, 157 (1965).
 - ²⁵N. C. Holmes, J. A. Moriaty, G. R. Gathers, and W. J. Nellis, *J. Appl. Phys.* **66**, 2962 (1989).
 - ²⁶F. Hajdu, *Acta Crystallogr., Sect. A: Cryst. Phys., Diffr., Theor. Gen. Crystallogr.* **28**, 250 (1972).
 - ²⁷K. Tsuji, K. Yaoita, M. Imai, O. Shimomura, and T. Kikegawa, *Rev. Sci. Instrum.* **60**, 2425 (1989).
 - ²⁸K. Funakoshi, Ph.D. thesis, Tokyo Institute of Technology, 1997.
 - ²⁹R. Kaplow, S. L. Strong, and B. L. Aberbach, *Phys. Rev.* **138**, A1336 (1965).
 - ³⁰W. Wagner and A. Pruß, *J. Phys. Chem. Ref. Data* **31**, 387 (2002).
 - ³¹A. P. Lyubartsev and A. Laaksonen, *Comput. Phys. Commun.* **128**, 565 (2000).
 - ³²H. J. C. Berendsen, J. R. Grigera, and T. P. Straatsma, *J. Phys. Chem.* **91**, 6269 (1987).
 - ³³K. Toukan and A. Rahman, *Phys. Rev. B* **31**, 2643 (1985).
 - ³⁴S. R. Elliott, *J. Chem. Phys.* **103**, 2758 (1995).
 - ³⁵D. R. Barker, M. Wilson, P. A. Madden, N. N. Medvedev, and A. Geiger, *Phys. Rev. E* **62**, 1427 (2000).
 - ³⁶Y. Waseda, *The Structure of Non-Crystalline Materials* (McGraw-Hill, New York, 1980).
 - ³⁷Y. Katayama and K. Tsuji, *J. Phys.: Condens. Matter* **15**, 6085 (2003).
 - ³⁸N. S. Gingrich and C. W. Tompson, *J. Chem. Phys.* **36**, 2398 (1962).
 - ³⁹R. J. Hemley, A. P. Jephcoat, H. K. Mao, C. S. Zha, L. W. Finger, and D. E. Cox, *Nature (London)* **330**, 737 (1987).
 - ⁴⁰W. F. Kuhs, J. L. Finny, C. Vettier, and D. V. Bliss, *J. Chem. Phys.* **81**, 3612 (1984).
 - ⁴¹G. W. Lee, W. J. Evans, and C.-S. Yoo, *Phys. Rev. B* **74**, 134112 (2006).
 - ⁴²J. A. Morrone and R. Car, *Phys. Rev. Lett.* **101**, 017801 (2008).
 - ⁴³I.-C. Lin, A. P. Seitsonen, M. D. Coutinho-Neto, I. Tavernelli, and U. Rothlisberger, *J. Phys. Chem. B* **113**, 1127 (2009).
 - ⁴⁴G. Weck, J. Eggert, P. Loubeyre, N. Desbiens, E. Bourasseau, J.-B. Maillet, M. Mezouar, and M. Hanfland, *Phys. Rev. B* **80**, 180202(R) (2009).